Neutrino observables in gauged $U(1)_{L_\alpha - L_\beta}$ models with two Higgs doublet and one singlet scalars*

Yuanchao Lou (娄元超)† Takaaki Nomura‡

College of Physics, Sichuan University, Chengdu 610065, China

Abstract: We discuss neutrino sector in models with two Higgs doublet and one singlet scalar fields under local $U(1)_{L_\alpha - L_\beta}$ symmetry. A neutrino mass matrix is formulated for these models via a type-I seesaw mechanism by introducing right-handed neutrinos. The neutrino mass matrix has more degrees of freedom than minimal scenarios that have only one new scalar field, but its structure is still restricted by symmetry. Subsequently, we find that the sum of neutrino mass can be lower than that of minimal scenarios and easily satisfies observed constraints. In addition, we can fit neutrino data for $U(1)_{L_e - L_{\mu(\tau)}}$ cases that are disfavored in minimal models. Furthermore, some correlations among sum of neutrino mass and CP violating phases are still observed, although we have more free parameters.

Keywords: neutrino mass, extended Higgs sector, new $U(1)$ gauge symmetry

DOI: 10.1088/1674-1137/adabce **CSTR:** 32044.14.ChinesePhysicsC.49053003

I. INTRODUCTION

The nature of neutrinos, such as non-zero masses and mixings, is one of the largest mysteries in particle physics. We must extend the standard model (SM) to generate neutrino masses, and an attractive appproach is the type-I seesaw mechanism, which introduces right-handed neutrinos [1−6], as a simple possibility. The new physics sector would have a more rich structure containing new particle contents in addition to right-handed neutrinos and/or new (gauge) symmetries. Thus, the compatibility among neutrino mass/mixing and new physics, particularly a flavor dependent symmetry, is important to explore.

An introduction of new $U(1)$ gauge symmetry provides simple extensions of the SM. Among many possibilities, local $U(1)_{L_\alpha - L_\beta}$ symmetries are interesting as they are anomaly free and the SM leptons have a flavor dependent charge $L_\alpha - L_\beta(\alpha,\beta = \{e,\mu,\tau\})$. Introducing such a symmetry restricts the structure of Yukawa interactions and the Majorana mass of right-handed neutrinos that are related to the neutrino mass structure. Compatibility among the $U(1)_{L_\alpha - L_\beta}$ symmetry and neutrino masses/mixings has been explored for the type-I seesaw scenario [7, 8], where one scalar field, $SU(2)_L$ singlet or doublet with non-zero $U(1)_{L_\alpha - L_\beta}$ charge, is introduced to develop a vacuum expectation values (VEVs) contributing to neutrino mass via Yukawa interaction as minimal choices[1)]. In this case, we have clear relations among neutrino observables and models are restricted by the current neutrino data [18]. Thus, only the $U(1)_{L_\mu - L_\tau}$ case with one singlet scalar having a charge ±1 can accommodate neutrino data when we consider constraints on sum of neutrino mass $\sum m_\nu \lesssim 0.12$ eV from CMB data by Planck [19] under the standard ΛCDM cosmological model. Remarkably, a more stringent constraint is obtained as $\sum m_\nu < 0.07$ eV (95%) if we include recent baryon acoustic oscillation (BAO) analysis by Dark Energy Spectroscopic Instrument (DESI) data [20]; even stronger bounds are estimated in Refs. [21, 22]. $U(1)_{L_\alpha - L_\beta}$ models are excluded when we add only one new scalar field and impose the constraint on the sum; it is marginal even if we consider $\sum m_\nu > 0.059$ eV prior leading bit looser constraint $\sum m_\nu < 0.113$. This analysis indicates that we must extend minimal $U(1)_{L_\alpha - L_\beta}$ models or modify the standard ΛCDM model. Thus, a next minimal case including both $SU(2)_L$ singlet and doublet scalar fields[2)] is worth consid-

Received 11 June 2024; Accepted 20 January 2025; Published online 21 January 2025

* Takaaki Nomura supported by the Fundamental Research Funds for the Central Universities

† E-mail: louyuanchao@stu.scu.edu.cn

‡ E-mail: nomura@scu.edu.cn

1) One can find other approaches, especially $U(1)_{L_\mu - L_\tau}$ case, discussing constrained neutrino mass matrix in other seesaw models including radiative mass generation [9−17].

2) Such a hybrid type is discussed in Ref. [23] to relax constraints regarding Z' boson. Also similar hybrid models are discussed in Refs. [24−27] for lepton flavor violation physics.

Content from this work may be used under the terms of the Creative Commons Attribution 3.0 licence. Any further distribution of this work must maintain attribution to the author(s) and the title of the work, journal citation and DOI. Article funded by SCOAP[3] and published under licence by Chinese Physical Society and the Institute of High Energy Physics of the Chinese Academy of Sciences and the Institute of Modern Physics of the Chinese Academy of Sciences and IOP Publishing Ltd

ering, and we investigate if we can still obtain some predictions in the neutrino sector satisfying the constraints on neutrino mass simultaneously.

In this paper, we discuss models with a local $U(1)_{L_\alpha - L_\beta}$ symmetry that introduce right-handed neutrinos and $SU(2)_L$ doublet and singlet scalars with non-zero charges under the new gauge symmetry. The models are characterized by the gauge symmetry and possible choices of charges for a doublet scalar field. We then explore neutrino masses and mixings in each model and search for parameters that can accommodate neutrino data. For allowed parameter sets, we show some predictions such as the sum of neutrino mass and CP violating phases.

The remainder of this paper is organized as follows. In Sec. II, we introduce models and formulate a scalar sector, neutral gauge bosons, charged lepton mass, and a neutrino mass matrix. In Sec. III, we show numerical analysis of neutrino masses, providing some predictions. Finally, we provide the conclusion and discussion in Sec. IV.

II. MODELS

In this section, we introduce models and formulate the neutrino mass matrix. The models are constructed under a framework of two Higgs doublet plus one singlet scalar under $U(1)_{L_\alpha - L_\beta}$ gauge symmetry. We also introduce three right-handed neutrinos charged under $U(1)_{L_\alpha - L_\beta}$ to achieve a type-I seesaw mechanism. In this scenario, one Higgs doublet H_1 has a charge of $Q_H = \pm 1$ and the singlet scalar has a charge of 1 under $U(1)_{L_\alpha - L_\beta}$. We summarize the charge assignments in Table 1. Note that $Q_H = \pm 1$ is also required to make the operator $\varphi H_1^\dagger H_2$(or $\varphi^* H_1^\dagger H_2$) gauge invariant to avoid a massless Goldstone boson from Higgs doublets. These assignments of the $U(1)_{L_\alpha - L_\beta}$ charge to scalar fields are the only relevant ones to obtain the neutrino mass matrix that can fit the neutrino data.

Table 1. Charge assignments of the leptons and scalar fields under $SU(2)_L \times U(1)_Y \times U(1)_{L_\alpha - L_\beta}$ where $L_{\alpha,\beta}$ corresponds to the lepton number for $\alpha(\beta) = \{e, \mu, \tau\}$ flavor $(\alpha \neq \beta)$ and $Q_H = +1$ or -1.

	L_{L_i}	e_{R_i}	ν_{R_i}	H_1	H_2	φ
$SU(2)_L$	2	1	1	2	2	1
$U(1)_Y$	$-\frac{1}{2}$	-1	0	1/2	1/2	0
$U(1)_{L_\alpha - L_\beta}$	$L_\alpha - L_\beta$	$L_\alpha - L_\beta$	$L_\alpha - L_\beta$	Q_H	0	1

The relevant Lagrangian for the lepton sector is given by

$$L_\ell = y_{\ell_1} \bar{L}_L e_R H_1 + y_{\ell_2} \bar{L}_L e_R H_2 + y_{\nu_1} \bar{L}_L \nu_R \tilde{H}_1 + y_{\nu_2} \bar{L}_L \nu_R \tilde{H}_2 + \frac{1}{2} M_0 \overline{\nu_R^c} \nu_R + \frac{1}{2} y_M \overline{\nu_R^c} \nu_R \varphi + \frac{1}{2} \tilde{y}_M \overline{\nu_R^c} \nu_R \varphi^* + h.c., \quad (1)$$

where $\tilde{H}_i = H_i^* \mathrm{i}\sigma_2$, with σ_2 being the second Pauli matrix, and the flavor index is omitted. The structure of Yukawa coupling matrices and a bare Majorana mass matrix are constrained by charge assignments under $U(1)_{L_\alpha - L_\beta}$, as discussed below. The scalar potential is also given by

$$\begin{aligned} V = & \ m_1^2 H_1^\dagger H_1 + m_2^2 H_2^\dagger H_2 + m_\varphi^2 |\varphi|^2 - (\mu \varphi^{(*)} H_1^\dagger H_2 + h.c.) \\ & + \lambda_1 (H_1^\dagger H_1)^2 + \lambda_2 (H_2^\dagger H_2)^2 + \lambda_\varphi |\varphi|^4 + \lambda_3 (H_1^\dagger H_1)(H_2^\dagger H_2) \\ & + \lambda_4 (H_1^\dagger H_2)(H_2^\dagger H_1) + \lambda_{H_1\varphi} (H_1^\dagger H_1)|\varphi|^2 + \lambda_{H_2\varphi} (H_2^\dagger H_2)|\varphi|^2, \end{aligned} \quad (2)$$

where φ or φ^* is determined by the $U(1)_{L_\alpha - L_\beta}$ charge of H_1 for the fourth term. In this work, we consider six models given in Table 2 that are distinguished by $U(1)$ symmetry and charge Q_H, providing us different structures of the neutrino mass matrix.

A. Scalar sector

Here, we review a scalar sector containing two Higgs doublets and one singlet scalar under extra $U(1)_{L_\alpha - L_\beta}$ gauge symmetry. The two Higgs doublets and singlet scalar are represented as

$$H_i = \begin{pmatrix} \phi_a^+ \\ \frac{1}{\sqrt{2}}(v_a + h_a + \mathrm{i}\eta_a) \end{pmatrix}, \quad \varphi = \frac{1}{\sqrt{2}}(\phi_R + v_\varphi + \mathrm{i}\phi_I), \quad (3)$$

where $a = 1, 2$, and v_a and v_φ are the VEVs of the corresponding fields. The VEVs can be obtained from the stationary conditions $(\partial V/\partial h_i)_0 = (\partial V/\partial \phi_R)_0 = 0$, where the subscript "0" indicates that all the component fields are taken to be zero. These conditions provide

$$\begin{aligned} & m_{H_1}^2 v_1 - m_{12}^2 v_2 + \frac{v_1}{2}(2v_1^2 \lambda_1 + v_2^2 \bar{\lambda} + v_\varphi^2 \lambda_{H_1\varphi}) = 0 \\ & m_{H_2}^2 v_2 - m_{12}^2 v_1 + \frac{v_2}{2}(2v_2^2 \lambda_2 + v_1^2 \bar{\lambda} + v_\varphi^2 \lambda_{H_2\varphi}) = 0 \\ & m_\varphi^2 v_\varphi - \frac{1}{\sqrt{2}} \mu v_1 v_2 + \lambda_\varphi v_\varphi^3 + \frac{\lambda_{H_1\varphi}}{2} v_1^2 v_\varphi + \frac{\lambda_{H_2\varphi}}{2} v_2^2 v_\varphi = 0, \end{aligned} \quad (4)$$

where $m_{12}^2 \equiv \mu v_\varphi / \sqrt{2}$ and $\bar{\lambda} = \lambda_3 + \lambda_4$.

The mass eigenstates for charged scalar components are obtained as in a two Higgs doublet model (THDM),

$$\begin{pmatrix} G^\pm \\ H^\pm \end{pmatrix} = \begin{pmatrix} \cos\beta & -\sin\beta \\ \sin\beta & \cos\beta \end{pmatrix} \begin{pmatrix} \phi_1^\pm \\ \phi_2^\pm \end{pmatrix}, \quad (5)$$

Table 2. Models distinguished by the extra $U(1)$ symmetry and H_1 charge Q_H.

	model (1)	model (2)	model (3)	model (4)	model (5)	model (6)
$U(1)_{L_i-L_j}$	L_e-L_μ	L_e-L_μ	L_e-L_τ	L_e-L_τ	$L_\mu-L_\tau$	$L_\mu-L_\tau$
Q_H	1	−1	1	−1	1	−1

where $\tan\beta = v_2/v_1$, $G^\pm$ corresponds to the Nambu-Goldstone (NG) boson absorbed by $W^\pm$, and $H^\pm$ is the physical charged Higgs boson. The mass of the charged Higgs boson can be expressed as

$$m^2_{H^\pm} = \frac{m^2_{12}}{\sin\beta\cos\beta} - \frac{v^2}{2}\lambda_4, \tag{6}$$

where $v = \sqrt{v_1^2+v_2^2} \simeq 246$ GeV.

Applying the conditions in Eq. (4), the mass matrix for CP-odd scalar bosons is obtained as

$$\mathcal{L} \in \frac{1}{2}\begin{pmatrix}\eta_1\\ \eta_2\\ \phi_I\end{pmatrix}^T \begin{pmatrix} \frac{\mu v_\varphi v_2}{\sqrt{2}v_1} & -\frac{\mu v_\varphi}{\sqrt{2}} & -\frac{\mu v_2}{\sqrt{2}} \\ -\frac{\mu v_\varphi}{\sqrt{2}} & \frac{\mu v_\varphi v_1}{\sqrt{2}v_2} & \frac{\mu v_1 v_2}{\sqrt{2}v_\varphi} \\ -\frac{\mu v_2}{\sqrt{2}} & \frac{\mu v_1}{\sqrt{2}} & \frac{\mu v_2}{\sqrt{2}} \end{pmatrix} \begin{pmatrix}\eta_1\\ \eta_2\\ \phi_I\end{pmatrix}. \tag{7}$$

This mass matrix can be diagonalized by rotating the basis as follows [28]:

$$\begin{pmatrix}\eta_1\\ \eta_2\\ \phi_I\end{pmatrix} = \begin{pmatrix} \frac{v_1}{v} & -\frac{v_\varphi v_2}{\sqrt{v_1^2v_2^2+v_\varphi^2v^2}} & \frac{v_1}{\sqrt{v_\varphi^2+v_1^2}} \\ \frac{v_2}{v} & -\frac{v_\varphi v_1}{\sqrt{v_1^2v_2^2+v_\varphi^2v^2}} & 0 \\ 0 & -\frac{v_1 v_2}{\sqrt{v_1^2v_2^2+v_\varphi^2v^2}} & \frac{v_\varphi}{\sqrt{v_\varphi^2+v_1^2}} \end{pmatrix} \begin{pmatrix}G_1^0\\ A^0\\ G_2^0\end{pmatrix}, \tag{8}$$

where $G^0_{1,2}$ represents a massless NG boson whose degrees of freedom are absorbed by Z and Z' bosons. Here, we note that the $\{\eta_1,\eta_2\}$ sector becomes THDM like in the limit of $v_\varphi \gg v$. The mass eigenvalue of physical CP-odd scalar boson A^0 is given by

$$m^2_{A^0} = \frac{m^2_{12}}{\sin\beta\cos\beta} + \frac{1}{\sqrt{2}}\frac{\mu v^2}{v_\varphi}. \tag{9}$$

Note that the mass of A^0 becomes zero when we take $\mu = 0$ because there is a spontaneously broken global $U(1)$ symmetry in the potential for the limit.

The CP-even scalar sector has three physical degrees of freedom $\{h_1,h_2,\phi_R\}$, and the mass matrix is given by

$$\mathcal{L} \supset \frac{1}{2}\begin{pmatrix}h_1\\ h_2\\ \phi_R\end{pmatrix}^T \begin{pmatrix} 2\lambda_1 v_1^2 + \frac{\mu v_\varphi v_2}{\sqrt{2}v_1} & \lambda_3 v_1 v_2 + \lambda_4 v_1 v_2 - \frac{\mu v_\varphi}{\sqrt{2}} & \eta\lambda_{H_1\varphi} v_1 - \frac{\mu v_2}{\sqrt{2}} \\ \lambda_3 v_1 v_2 + \lambda_4 v_1 v_2 - \frac{\mu v_\varphi}{\sqrt{2}} & 2\lambda_2 v_2^2 + \frac{\mu v_1 v_\varphi}{\sqrt{2}v_2} & v_\varphi \lambda_{H_2\varphi} v_2 - \frac{\mu v_1}{\sqrt{2}} \\ v_\varphi\lambda_{H_1\varphi} v_1 - \frac{\mu v_2}{\sqrt{2}} & v_\varphi\lambda_{H_2\varphi} v_2 - \frac{\mu v_1}{\sqrt{2}} & 2v_\varphi^2\lambda_\varphi + \frac{\mu v_1 v_2}{\sqrt{2}\varphi} \end{pmatrix} \begin{pmatrix}h_1\\ h_2\\ \phi_R\end{pmatrix}, \tag{10}$$

where we impose conditions in Eq. (4). This mass matrix can be diagonalized using a 3×3 orthogonal matrix providing three physical mass eigenvalues. Such an orthogonal matrix R with three Euler parameters $\{\alpha_1,\alpha_2,\alpha_3\}$ is given by

$$R(\alpha_1,\alpha_2,\alpha_3) = \begin{pmatrix} c_{\alpha_1}c_{\alpha_2} & -s_{\alpha_1}c_{\alpha_2} & s_{\alpha_2} \\ -c_{\alpha_1}s_{\alpha_2}s_{\alpha_3} + s_{\alpha_1}c_{\alpha_3} & c_{\alpha_1}c_{\alpha_3} + s_{\alpha_1}s_{\alpha_2}s_{\alpha_3} & c_{\alpha_2}s_{\alpha_3} \\ -c_{\alpha_1}s_{\alpha_2}c_{\alpha_3} - s_{\alpha_1}s_{\alpha_3} & -c_{\alpha_1}s_{\alpha_3} + s_{\alpha_1}s_{\alpha_2}c_{\alpha_3} & c_{\alpha_2}c_{\alpha_3} \end{pmatrix}, \tag{11}$$

where $c_{\alpha_i} = \cos\alpha_i (s_{\alpha_i} = \sin\alpha_i)$. Thus, mass eigenstates are obtained such that

$$\begin{pmatrix}h_1\\ h_2\\ \phi_R\end{pmatrix} = R_{ij}\begin{pmatrix}H^0\\ h^0\\ \xi^0\end{pmatrix}_j. \tag{12}$$

In this work, we do not discuss further details of the scalar sector as our focus is on the neutrino sector. Thus, we simply assume that parameters in the scalar potential are selected to satisfy phenomenological constraints regarding Higgs boson physics.

B. Neutral gauge bosons

Here, we focus on the neutral gauge boson sector in the model because the charged gauge boson $W^{\pm}$ is the same as the SM one. After spontaneous symmetry breaking, we obtain the mass terms

$$\mathcal{L}_M = \frac{1}{2}m_{Z_{\rm SM}}^2\tilde{Z}_\mu\tilde{Z}^\mu + \frac{1}{2}\tilde{m}_{Z'}^2\tilde{Z}'_\mu\tilde{Z}'^\mu + \Delta M^2\tilde{Z}_\mu\tilde{Z}'^\mu, \tag{13}$$

where $m_{Z_{\rm SM}}^2 = v^2(g_1^2+g_2^2)/4$ with $g_{1(2)}$ being $U(1)_Y(SU(2)_L)$ gauge coupling, $\tilde{m}_{Z'}^2 = g_X^2(v_\varphi^2+v_1^2)$ with new gauge coupling g_X, and $\Delta M^2 = g_X\sqrt{g_1^2+g_2^2}v_1^2/2$. Here, $\tilde{Z}_\mu = \cos\theta_W W_\mu^3 - \sin\theta_W B_\mu$ where W_μ^3 and B_μ result from $SU(2)_L$ and $U(1)_Y$ gauge fields as in the SM, whereas $\tilde{Z}'_\mu$ is $U(1)_{L_\alpha-L_\beta}$ gauge field. Note that we do not consider kinetic mixing among the $U(1)$ gauge fields assuming it is negligibly small. Thus, we can diagonalize the mass terms by rotating the fields and obtain mass eigenstates

$$\begin{pmatrix} Z \\ Z' \end{pmatrix} = \begin{pmatrix} \cos\chi & \sin\chi \\ -\sin\chi & \cos\chi \end{pmatrix}\begin{pmatrix} \tilde{Z} \\ \tilde{Z}' \end{pmatrix}, \tag{14}$$

$$\tan 2\chi = \frac{2\Delta M^2}{m_{Z_{\rm SM}}^2 - \tilde{m}_{Z'}^2}. \tag{15}$$

The mass eigenvalues are also obtained as

$$m_{Z,Z'}^2 = \frac{1}{2}(m_{Z_{\rm SM}}^2 + \tilde{m}_{Z'}^2) \pm \frac{1}{2}\sqrt{(m_{Z_{\rm SM}}^2 - \tilde{m}_{Z'}^2)^2 + 4\Delta M^4}. \tag{16}$$

Here, we briefly discuss the constraints on Z-Z' mixing from an electroweak precision test (EWPT). The mixing is typically constrained as $|\sin\chi| \lesssim 10^{-3}-10^{-4}$ when the Z' boson is obtained from local $U(1)$ symmetry as a subgroup of GUT symmetry such as $SO(10)$ and E_6 [29]. The EWPT constraint is discussed for $U(1)_{L_\mu-L_\tau}$ in Ref. [27], where we find $-0.0008 \lesssim g_X\sin\chi \lesssim 0.0003$. We apply the constraint as a reference under a $m_Z^2 \ll m_{Z'}^2$ mass hierarchy for neutral gauge bosons. In our case, the constraint approximately becomes

$$\frac{g_X^2 m_Z v\cos\beta}{m_{Z'}^2} \lesssim 8\times10^{-4}. \tag{17}$$

In Fig. 1, we show the region excluded by the EWPT for $U(1)_{L_\mu-L_\tau}$ with $\tan\beta = 5$. We observe that $O(1)$ gauge coupling is allowed if Z' mass satisfies 1700 GeV $\lesssim m_{Z'}$, where the allowed region is also safe from other experimental constraints. We expect a similar Z-Z' mixing constraint in the other cases, $U(1)_{L_e-L_\mu}$ and $U(1)_{L_e-L_\tau}$. This constraint restricts $v_\varphi \simeq m_{Z'}/g_X$ and can affect the Majorana mass of ν_R. However, it does not provide much impact in fitting the neutrino mass because we also have Yukawa couplings that are free parameters. In our analysis below, we consider a heavy Z' and assume Z-Z' mixing is negligibly small to avoid the EWPT.

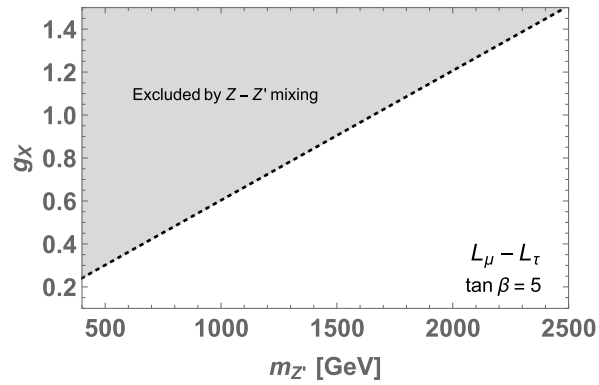

Fig. 1. Gray region is excluded by the EWPT for $U(1)_{L_\mu-L_\tau}$ with $\tan\beta = 5$.

C. Charged lepton mass

The mass matrix of the charged lepton is generated via Yukawa interactions in Eq. (1) after electroweak symmetry breaking. Thus, the mass term is given by

$$\overline{\ell_L}(M_e)_{\ell\ell'}\ell'_R + h.c. = \overline{\ell_L}\left(\frac{v_1}{\sqrt{2}}y_{\ell_1} + \frac{v_2}{\sqrt{2}}y_{\ell_2}\right)_{\ell\ell'}\ell'_R + h.c., \tag{18}$$

where $\ell(\ell') = \{e,\mu,\tau\}$. Generally, the mass matrix is not diagonal and its structure depends on the model. The possible structures of matrix M_e are as follows

$$M_e^{\rm Model(1)}: \begin{pmatrix} \times & 0 & \times \\ 0 & \times & 0 \\ 0 & \times & \times \end{pmatrix}, \quad M_e^{\rm Model(2)}: \begin{pmatrix} \times & 0 & 0 \\ 0 & \times & \times \\ \times & 0 & \times \end{pmatrix},$$
$$M_e^{\rm Model(3)}: \begin{pmatrix} \times & \times & 0 \\ 0 & \times & \times \\ 0 & 0 & \times \end{pmatrix}, \quad M_e^{\rm Model(4)}: \begin{pmatrix} \times & 0 & 0 \\ \times & \times & 0 \\ 0 & \times & \times \end{pmatrix},$$
$$M_e^{\rm Model(5)}: \begin{pmatrix} \times & 0 & \times \\ \times & \times & 0 \\ 0 & 0 & \times \end{pmatrix}, \quad M_e^{\rm Model(6)}: \begin{pmatrix} \times & \times & 0 \\ 0 & \times & 0 \\ \times & 0 & \times \end{pmatrix}, \tag{19}$$

where $\times$ indicates a non-zero element. The mass matrix can be diagonalized using bi-unitary matrices V_{eL} and V_{eR} transforming ℓ_L and ℓ_R; $M_d^{\rm diagonal} = V_{eL}^\dagger M_e V_{eR}$. Note that such a transformation induces a flavor-changing neutral current (FCNC) for the interaction among Z' and leptons owing to lepton flavor dependent charges, and it is

strongly constrained by LFV search experiments [8]. Here, we illustrate an LFV constraint in a simple case. First, the Z' interaction for charged leptons is given by

$$\mathcal{L}_{Z'\ell\bar{\ell}} = g_X Z'_\mu \left[\overline{\ell_L} V^\dagger_{eL} Q_{L_\alpha-L_\beta} V_{eL}\gamma^\mu \ell_L + \overline{\ell_R} V^\dagger_{eR} Q_{L_\alpha-L_\beta} V_{eR}\gamma^\mu \ell_R\right], \tag{20}$$

where $Q_{L_\alpha-\beta}$ indicates a diagonal matrix whose elements are $L_\alpha - L_\beta$ charge, *e.g.* $Q_{L_e-L_\mu} = (1,-1,0)$. The FCNC appears when $V^\dagger_{eL(eR)} Q_{L_\alpha-L_\beta} V_{eL(eR)}$ is not a diagonal matrix. As an example, we consider M_e of model (3) in Eq. (19) with $(M_e)_{23} = 0$ for simplicity. Subsequently, focusing on e-μ sector, the mass matrix is expressed by

$$M_e^{e\mu} = \begin{pmatrix} M_e & \delta m \\ 0 & M_\mu \end{pmatrix}. \tag{21}$$

Selecting $\delta m \ll M_\mu$, this matrix can be approximately diagonalized by

$$V^\dagger_{eL} M_e^{e\mu} V_{eR} \sim \begin{pmatrix} m_e & 0 \\ 0 & m_\mu \end{pmatrix},$$
$$V_{eL} \sim \begin{pmatrix} 1 & \frac{\delta m}{M_\mu} \\ -\frac{\delta m}{M_\mu} & 1 \end{pmatrix}, \quad V_{eR} \sim \mathbf{1}, \tag{22}$$

where $m_e \sim M_e$ and $m_\mu \sim M_\mu$. Because model (3) is the $U(1)_{L_e-L_\tau}$ case, the LFV interaction is approximately given by

$$g_X \frac{\delta m}{m_\mu} Z'_\mu [\bar{\mu}\gamma^\mu P_L e + \bar{e}\gamma^\mu P_L \mu]. \tag{23}$$

Thus, the experimental constraint for $\mu \to ee\bar{e}$ process is the most stringent one for the heavy Z' case[1)]; it is induced via a virtual Z' as $\mu \to eZ'^* \to ee\bar{e}$. We can estimate the decay width and branching ratio (BR) as

$$\Gamma_{\mu\to ee\bar{e}} \simeq \frac{g_X^4}{8m_{Z'}^4}\left(\frac{\delta m}{m_\mu}\right)^2 \frac{m_\mu^5}{192\pi^3}, \tag{24}$$

$$BR(\mu \to ee\bar{e}) \simeq \frac{g_X^4}{g_2^2 G_F^2 m_{Z'}^4}\left(\frac{\delta m}{m_\mu}\right)^2, \tag{25}$$

where G_F is the Fermi constant. Applying the current limit $BR(\mu \to ee\bar{e}) \lesssim 10^{-12}$, we obtain

$$g_X^4 \left(\frac{\delta m}{m_\mu}\right)^2 \left(\frac{\text{TeV}}{m_{Z'}}\right)^4 \lesssim 6\times 10^{-11}. \tag{26}$$

Thus, $\delta m/m_\mu$ should be very small as $\delta m/m_\mu \lesssim O(10^{-5})$ when $g_X = O(1)$, and $m_{Z'}$ is the TeV scale. Note that we will obtain looser constraints when we consider the LFV decay of an τ lepton. In the numerical analysis below, we assume that off-diagonal elements of the matrix is negligibly small and $V_{eL(eR)} \simeq 1$ for simplicity.

D. Neutrino mass

After spontaneous symmetry breaking, we obtain the Dirac mass M_D between ν_L and ν_R ($\overline{\nu_L} M_D \nu_R$) and the Majorana mass M_R of ν_R. These mass matrices are given by

$$M_D = \frac{y_{\nu_1} v_1}{\sqrt{2}} + \frac{y_{\nu_2} v_2}{\sqrt{2}}, \tag{27}$$

$$M_R = M_0 + \frac{y_M v_\varphi}{\sqrt{2}} + \frac{\tilde{y}_M v_\varphi}{\sqrt{2}}. \tag{28}$$

The structure of these matrices differs for each model. For M_D, we determine the structure as follows:

$$M_D^{\text{Model}(1)}: \begin{pmatrix} \times & 0 & 0 \\ 0 & \times & \times \\ \times & 0 & \times \end{pmatrix}, \quad M_D^{\text{Model}(2)}: \begin{pmatrix} \times & 0 & \times \\ 0 & \times & 0 \\ 0 & \times & \times \end{pmatrix},$$
$$M_D^{\text{Model}(3)}: \begin{pmatrix} \times & 0 & 0 \\ \times & \times & 0 \\ 0 & \times & \times \end{pmatrix}, \quad M_D^{\text{Model}(4)}: \begin{pmatrix} \times & \times & 0 \\ 0 & \times & \times \\ 0 & 0 & \times \end{pmatrix},$$
$$M_D^{\text{Model}(5)}: \begin{pmatrix} \times & \times & 0 \\ 0 & \times & 0 \\ \times & 0 & \times \end{pmatrix}, \quad M_D^{\text{Model}(6)}: \begin{pmatrix} \times & 0 & \times \\ \times & \times & 0 \\ 0 & 0 & \times \end{pmatrix}. \tag{29}$$

We also determine the structure of M_R for each model such that

$$M_R^{\text{Model}(1,2)}: \begin{pmatrix} 0 & \times & \times \\ \times & 0 & \times \\ \times & \times & \times \end{pmatrix}, \quad M_R^{\text{Model}(3,4)}: \begin{pmatrix} 0 & \times & \times \\ \times & \times & \times \\ \times & \times & 0 \end{pmatrix},$$
$$M_R^{\text{Model}(5,6)}: \begin{pmatrix} \times & \times & \times \\ \times & 0 & \times \\ \times & \times & 0 \end{pmatrix}, \tag{30}$$

1) The case of light Z' allowing $\ell_i \to \ell_j Z'$ decay is discussed in Ref. [8] providing tighter constraints.

where the structure is the same when a gauge symmetry of the models is identical.

The neutrino mass in type-I seesaw model is given by

$$m_\nu = -M_D M_R^{-1} M_D^T. \tag{31}$$

We then express the active neutrino mass matrix as

$$m_\nu = \kappa \tilde{m}_\nu, \tag{32}$$

where κ has a mass dimension, and $\tilde{m}_\nu$ is dimensionless. The neutrino mass matrix m_ν is diagonalized using a unitary matrix V_ν via $D_\nu = |\kappa|\tilde{D}_\nu = V_\nu^T m_\nu V_\nu = |\kappa| V_\nu^T \tilde{m}_\nu V_\nu$. Thus, $|\kappa|$ is determined by

$$(\mathrm{NO}):\ |\kappa|^2 = \frac{|\Delta m^2_{\rm atm}|}{\tilde{D}^2_{\nu_3} - \tilde{D}^2_{\nu_1}}, \quad (\mathrm{IO}):\ |\kappa|^2 = \frac{|\Delta m^2_{\rm atm}|}{\tilde{D}^2_{\nu_2} - \tilde{D}^2_{\nu_3}}, \tag{33}$$

where $\Delta m^2_{\rm atm}$ is atmospheric neutrino mass-squared splitting, and NO and IO represent the normal and inverted orderings, respectively, of neutrino mass eigenvalues. Subsequently, the solar mass squared splitting can be expressed in terms of $|\kappa|$ as follows:

$$\Delta m^2_{\rm sol} = |\kappa|^2 (\tilde{D}^2_{\nu_2} - \tilde{D}^2_{\nu_1}), \tag{34}$$

which can be compared with the observed value. The observed mixing matrix is defined by $U = V_{eL}^\dagger V_\nu$ [1)], where it is parametrized using three mixing angles $\theta_{ij} (i, j = 1, 2, 3; i < j)$, one CP violating Dirac phase δ_{CP}, and two Majorana phases α_{21}, α_{31} as follows:

$$U = \begin{pmatrix} c_{12}c_{13} & s_{12}c_{13} & s_{13}e^{-i\delta_{CP}} \\ -s_{12}c_{23} - c_{12}s_{23}s_{13}e^{i\delta_{CP}} & c_{12}c_{23} - s_{12}s_{23}s_{13}e^{i\delta_{CP}} & s_{23}c_{13} \\ s_{12}s_{23} - c_{12}c_{23}s_{13}e^{i\delta_{CP}} & -c_{12}s_{23} - s_{12}c_{23}s_{13}e^{i\delta_{CP}} & c_{23}c_{13} \end{pmatrix} \begin{pmatrix} 1 & 0 & 0 \\ 0 & e^{i\alpha_{21}/2} & 0 \\ 0 & 0 & e^{i\alpha_{31}/2} \end{pmatrix}. \tag{35}$$

Here, c_{ij} and s_{ij} denote $\cos\theta_{ij}$ and $\sin\theta_{ij}$ $(i, j = 1-3)$, respectively. Matrix U is identified as the Pontecorvo-Maki-Nakagawa-Sakata (PMNS) matrix [30, 31]. Each of the mixings is given in terms of the component of U as follows:

$$\sin^2\theta_{13} = |U_{e3}|^2,$$
$$\sin^2\theta_{23} = \frac{|U_{\mu3}|^2}{1-|U_{e3}|^2},$$
$$\sin^2\theta_{12} = \frac{|U_{e2}|^2}{1-|U_{e3}|^2}. \tag{36}$$

The Dirac phase $\delta_{\rm CP}$ is given by computing the Jarlskog invariant as follows:

$$\sin\delta_{\rm CP} = \frac{{\rm Im}[U_{e1}U_{\mu2}U^*_{e2}U^*_{\mu1}]}{s_{23}c_{23}s_{12}c_{12}s_{13}c^2_{13}},$$
$$\cos\delta_{\rm CP} = -\frac{|U_{\tau1}|^2 - s^2_{12}s^2_{23} - c^2_{12}c^2_{23}s^2_{13}}{2c_{12}s_{12}c_{23}s_{23}s_{13}}, \tag{37}$$

where $\delta_{\rm CP}$ be subtracted from π if $\cos\delta_{\rm CP}$ is negative. The Majorana phases α_{21}, α_{31} are determined as

$$\sin\left(\frac{\alpha_{21}}{2}\right) = \frac{{\rm Im}[U^*_{e1}U_{e2}]}{c_{12}s_{12}c^2_{13}}, \quad \cos\left(\frac{\alpha_{21}}{2}\right) = \frac{{\rm Re}[U^*_{e1}U_{e2}]}{c_{12}s_{12}c^2_{13}}, \tag{38}$$

$$\sin\left(\frac{\alpha_{31}}{2} - \delta_{\rm CP}\right) = \frac{{\rm Im}[U^*_{e1}U_{e3}]}{c_{12}s_{13}c_{13}},$$
$$\cos\left(\frac{\alpha_{31}}{2} - \delta_{\rm CP}\right) = \frac{{\rm Re}[U^*_{e1}U_{e3}]}{c_{12}s_{13}c_{13}}, \tag{39}$$

where $\alpha_{21}/2$, $\alpha_{31}/2 - \delta_{\rm CP}$ are subtracted from π, when $\cos\left(\frac{\alpha_{21}}{2}\right)$, $\cos\left(\frac{\alpha_{31}}{2} - \delta_{\rm CP}\right)$ are negative. In addition, the effective mass for the neutrinoless double beta decay is given by

$$\langle m_{ee}\rangle = |\kappa||\tilde{D}_{\nu_1}\cos^2\theta_{12}\cos^2\theta_{13} + \tilde{D}_{\nu_2}\sin^2\theta_{12}\cos^2\theta_{13}e^{i\alpha_{21}} + \tilde{D}_{\nu_3}\sin^2\theta_{13}e^{-2i\delta_{\rm CP}}|, \tag{40}$$

where its observed value could be tested in experiments such as KamLAND-Zen [32], LEGEND [33], and nEXO [34].

III. NUMERICAL ANALYSIS

In this section, we discuss neutrino observables such

1) We can approximate $V_{eL} \simeq 1$ to suppress LFV as discussed in previous subsection.

as masses, mixings, and CP-phases in our models. These values are numerically estimated because structures of the neutrino mass matrix are too complex to obtain analytic solutions for neutrino observables. In the numerical calculation, we modify the neutrino mass matrix as

$$m_\nu = -\frac{(M_D)_{11}^2}{(M_R)_{kk}} \tilde{M}_D \tilde{M}_R^{-1} \tilde{M}_D^T, \tag{41}$$

where $\tilde{M}_D \equiv M_D/(M_D)_{11}$ and $\tilde{M}_R = M_R/(M_R)_{kk}$ with $(M_R)_{kk}$ being a non-zero diagonal element of M_R in Eq. (30). The scaling factor $\frac{(M_D)_{11}^2}{(M_R)_{kk}}$ is identified as κ in Eq. (32) that will be evaluated using Eq. (33). Subsequently, we scan the elements of $\tilde{M}_D$ and $\tilde{M}_R$ in the range of

$$\left|(\tilde{M}_{D,R})_{ij}\right| \in [0.1, 10], \quad \left((\tilde{M}_D)_{11} = 1, \quad (\tilde{M}_R)_{kk} = 1\right) \tag{42}$$

where we consider these matrix elements do not have large hierarchy. Note that the elements are generally complex, and we remove phases of diagonal elements of matrix M_D by redefining phases of lepton fields without loss of generality. The neutrino observables are numerically estimated using the formulas in the previous section to explore the tendency in each model. In the analysis, we adopt NuFit 5.2 neutrino data [18] for the values of $\{\sin\theta_{12}, \sin\theta_{23}, \sin\theta_{13}, \Delta m^2_{\rm atm}, \Delta m^2_{\rm sol}\}$ within the 3σ range as

$$\begin{aligned}
&0.270 < \sin^2\theta_{12} < 0.341, \quad 0.406 < \sin^2\theta_{23} < 0.620,\\
&0.02029 < \sin^2\theta_{13} < 0.02391,\\
&2.428\times10^{-3}\ {\rm eV}^2 < |\Delta m^2_{\rm sol}| < 2.597\times10^{-3}\ {\rm eV}^2,\\
&6.82\times10^{-5}\ {\rm eV}^2 < \Delta m^2_{\rm sol} < 8.03\times10^{-5}\ {\rm eV}^2.
\end{aligned} \tag{43}$$

Subsequently, we search for values of $(\tilde{M}_{D,R})_{ij}$ reproducing these 3σ ranges of the observables. Here, we focus on the NO case and check if we can obtain the sum of neutrino masses $\sum m_\nu$ satisfying the constraint of CMB+DESI, $\sum m_\nu < 70$ meV. As a result, we find that models (2) and (4) are disfavored to fit the neutrino data within 3σ, whereas the other models have allowed parameter sets to fit the data. Additionally, we do not have a clear correlation between neutrino mixing angles and the other observables owing to increased free parameters compared with minimal scenarios. For the allowed models, we show some observables such as sum of masses and phases as our predictions.

In Fig. 2, we show $\langle m_{ee}\rangle$ and m_1 (the lightest neutrino mass) for the allowed parameter points in each model. The horizontal lines shows the current constraint from KamLand-Zen [32] and the future prospect in nEXO [34] with energy-density functional (EDF) theory for the nuclear matrix element. The distributions are almost similar in these models and some points can be tested in future

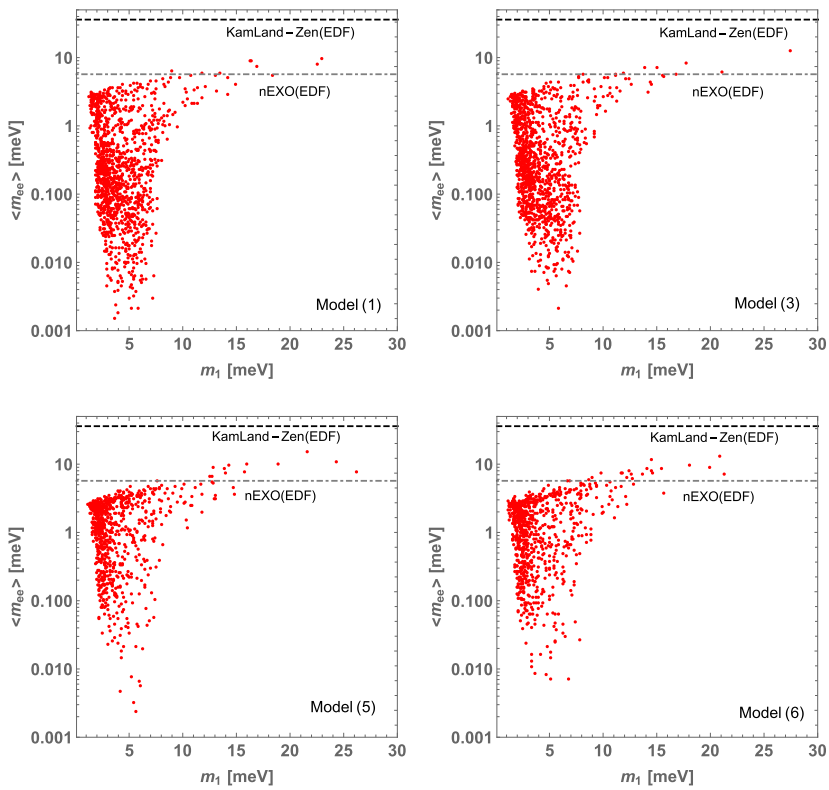

Fig. 2. (color online) Predicted values on the $\{m_1, \langle m_{ee}\rangle\}$ plane for allowed parameter points in each model.

neutrinoless double beta decay experiments.

In Fig. 3, we show $\sum m_\nu$ and $\delta_{\rm CP}$ for the allowed parameter points in each model. The vertical line indicates the upper limit using CMB+DESI data. We find a correlation between $\sum m_\nu$ and $\delta_{\rm CP}$ where models (1) and (6) [(3) and (5)] exhibit similar behavior. They exhibit ditinguishable behavior in which one tends to provide a small $\sum m_\nu$ at $\delta_{\rm CP}\sim 200^\circ$, and the other one tends to provide a small $\sum m_\nu$ at $\delta_{\rm CP}\sim 0^\circ(360^\circ)$. We also indicate the $1(3)\sigma$ range of the $\delta_{\rm CP}$ value in the light-blue (cyan) region. These two types of distributions can be distinguished if we have more precision for $\sum m_\nu$ and $\delta_{\rm CP}$ in the future.

Figures 4 and 5 show $\delta_{\rm CP}$-α_{21} and $\delta_{\rm CP}$-α_{31} values for the allowed parameter points in each model. We find some correlations among phases, where the correlations of $\delta_{\rm CP}$-α_{21} in models (1) and (6) [(3) and (5)] exhibit similar behavior. In each case, the value of α_{21} is concentrated around 100−250 degrees. In contrast, the correlations of $\delta_{\rm CP}$-α_{31} are different in each model. In these plots, we show the $1(3)\sigma$ range of $\delta_{\rm CP}$ in the light-blue region similar to Fig. 3. In addition, we also show the correlation between α_{21} and α_{31} in Fig. 6, where models (1) and (6) [(3) and (5)] exhibit a similar behavior.

IV. SUMMARY AND DISCUSSION

We have discussed neutrino observables in $U(1)_{L_\alpha-L_\beta}$ models, for which we introduce two Higgs doublet and one singlet scalar fields with non-zero charges under new $U(1)$ as extensions of minimal models that have only one new scalar field. The six models are characterized by the choice of $U(1)_{L_\alpha-L_\beta}$ gauge symmetry and its charge assignment to the two Higgs doublet. We have then formulated a scalar sector, neutral gauge bosons, a charged lepton mass matrix, and a neutrino mass matrix in the models. The structure of neutrino mass matrix is still restricted by the gauge symmetry but the number of free parameters is increased compared with minimal cases.

In this work, we have focused on the neutrino sector and numerically analyzed neutrino observables. Subsequently, we have determined four models can fit the current neutrino data in 3σ and satisfy constraints on the sum of neutrino mass including recent DESI and Planck data for normal ordering that excludes minimal models under the ΛCDM cosmological model. Although we do not have a correlation between the neutrino mixing angle and other observable because of increased free parameters, we have found some correlations between some observables such as the sum of the neutrino mass and CP phases. In particular, we have found two types of distin-

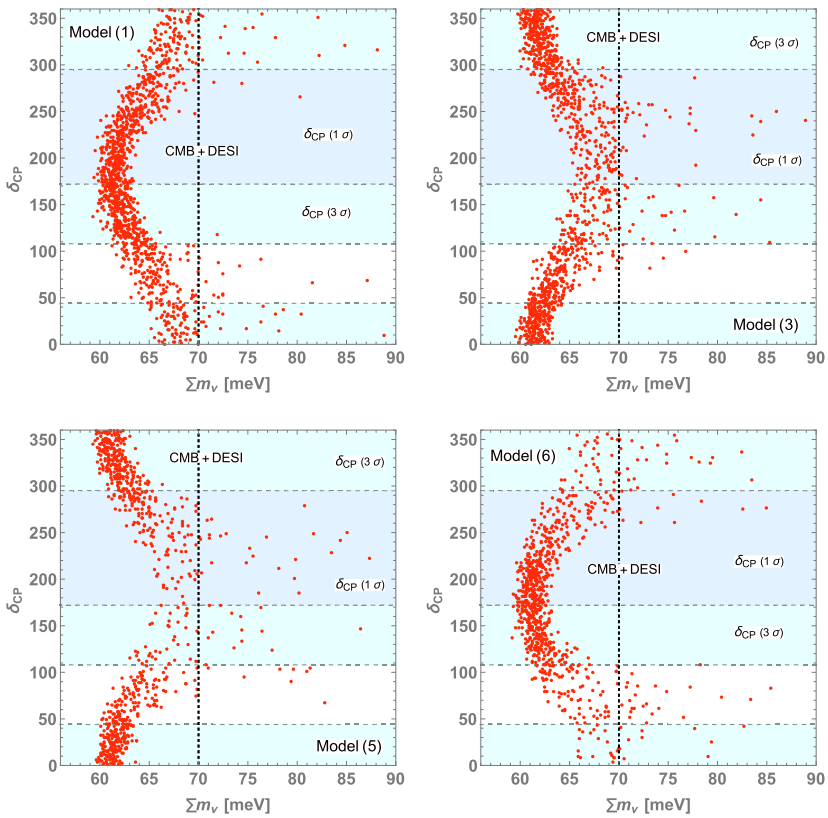

Fig. 3. (color online) Predicted values on the $\{\sum m_\nu, \delta_{\rm CP}\}$ plane for allowed parameter points in each model. The light-blue (cyan) region indicates $1(3)\sigma$ range of $\delta_{\rm CP}$ value.

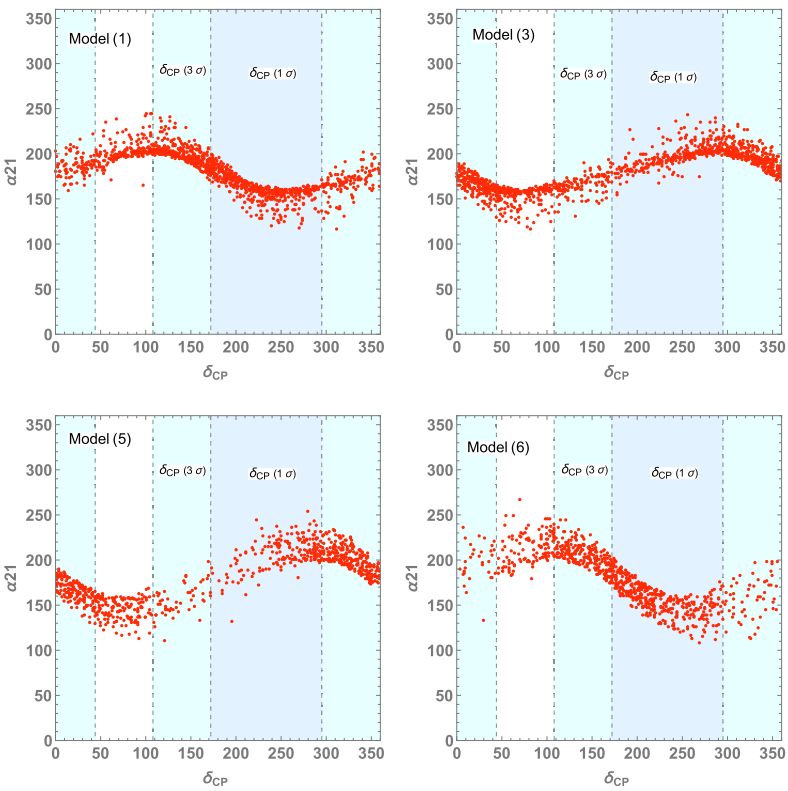

Fig. 4. (color online) Predicted values on the $\{\delta_{\rm CP}, \alpha_{21}\}$ plane for allowed parameter points in each model. The light-blue (cyan) region also indicates 1(3)σ range of the $\delta_{\rm CP}$ value.

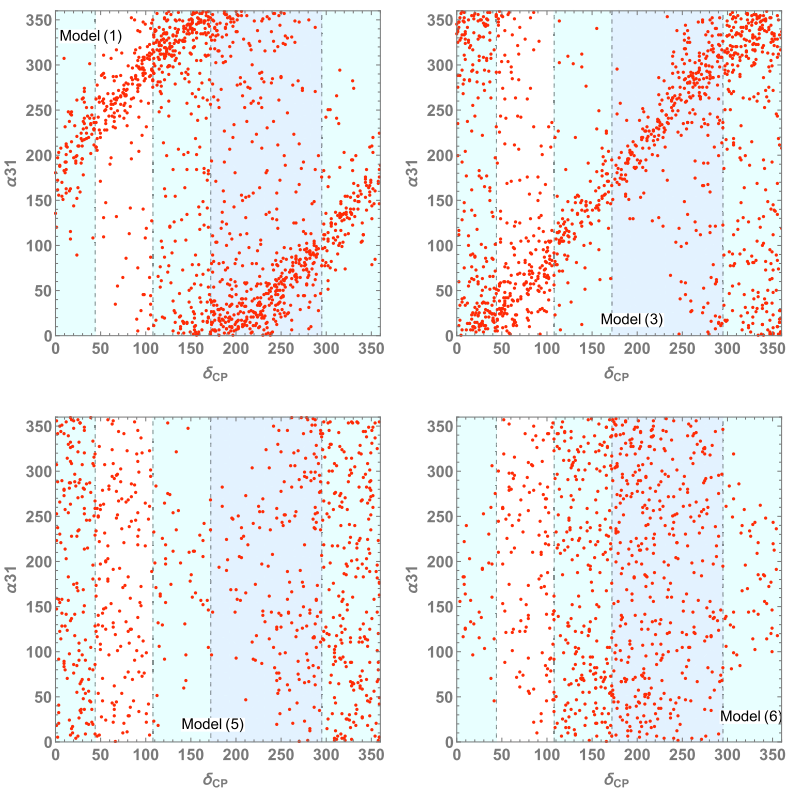

Fig. 5. (color online) Predicted values on the $\{\delta_{\rm CP}, \alpha_{31}\}$ plane for allowed parameter points in each model. The light-blue (cyan) region is the same as in Fig. 4.

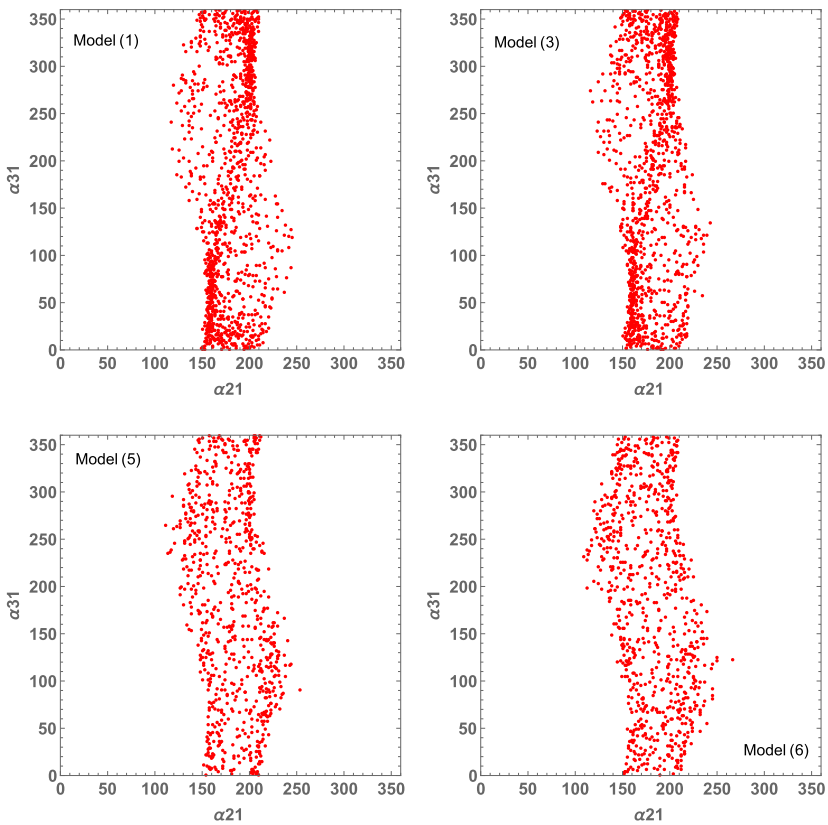

Fig. 6. (color online) Predicted values on the $\{\alpha_{21},\alpha_{31}\}$ plane for allowed parameter points in each model.

guishable distributions on the $\{\sum m_\nu,\delta_{\rm CP}\}$ plane that can be tested in the future to increase the precision for these observables. Some correlations are also observed among CP phases, although measuring them directly is difficult. To further distinguish the models, we would require to explore Higgs and Z' physics, for example, searching for collider signals that are specific in the models. The analysis of these physics is beyond the scope of this paper and it is left for future works.

References

[1] P. Minkowski, Phys. Lett. B **67**, 421 (1977)
[2] T. Yanagida, Conf. Proc. C **7902131**, 95-99 KEK-79-18-95, 1979
[3] T. Yanagida, Phys. Rev. D **20**, 2986 (1979)
[4] M. Gell-Mann, P. Ramond, and R. Slansky, arXiv: 1306.4669[hep-th]
[5] R. N. Mohapatra and G. Senjanovic, Phys. Rev. Lett. **44**, 912 (1980)
[6] J. Schechter and J. W. F. Valle, Phys. Rev. D **22**, 2227 (1980)
[7] K. Asai, K. Hamaguchi, and N. Nagata, Eur. Phys. J. C **77**(11), 763 (2017), arXiv: 1705.00419[hep-ph]
[8] K. Asai, K. Hamaguchi, N. Nagata *et al.*, Phys. Rev. D **99**(5), 055029 (2019), arXiv: 1811.07571[hep-ph]
[9] S. Baek, H. Okada, and K. Yagyu, JHEP **2015**, 049 (2015), arXiv: 1501.01530[hep-ph]
[10] S. Lee, T. Nomura, and H. Okada, Nucl. Phys. B **931**, 179 (2018), arXiv: 1702.03733[hep-ph]
[11] C. H. Chen and T. Nomura, Nucl. Phys. B **940**, 292 (2019), arXiv: 1705.10620[hep-ph]
[12] T. Nomura and H. Okada, Phys. Rev. D **97**(9), 095023 (2018), arXiv: 1803.04795[hep-ph]
[13] T. Nomura and H. Okada, Phys. Lett. B **783**, 381 (2018), arXiv: 1805.03942[hep-ph]
[14] K. Asai, Eur. Phys. J. C **80**(2), 76 (2020), arXiv: 1907.04042[hep-ph]
[15] T. Araki, K. Asai, J. Sato *et al.*, Phys. Rev. D **100**(9), 095012 (2019), arXiv: 1909.08827[hep-ph]
[16] M. Bauer, P. Foldenauer, and M. Mosny, Phys. Rev. D **103**(7), 075024 (2021), arXiv: 2011.12973[hep-ph]
[17] T. Nomura and H. Okada, Phys. Lett. B **848**, 138393 (2024), arXiv: 2304.03905[hep-ph]
[18] I. Esteban, M. C. Gonzalez-Garcia, M. Maltoni *et al.*, JHEP **2020**, 178 (2020), arXiv: 2007.14792 [hep-ph]
[19] N. Aghanim *et al.* (Planck) Astron. Astrophys. **641**, 67 (2020), [Erratum: Astron. Astrophys. 652, 3 (2021)], arXiv: 1807.06209 [astro-ph.CO]
[20] A. G. Adame *et al.* (DESI), arXiv: 2404.03002 [astro-ph.CO]
[21] N. Craig, D. Green, J. Meyers *et al.*, arXiv: 2405.00836 [astro-ph.CO]
[22] D. Wang, O. Mena, E. Di Valentino *et al.*, arXiv:

2405.03368 [astro-ph.CO]
[23] K. Asai, C. Miyao, S. Okawa *et al*., arXiv: 2401.17613 [hep-ph]
[24] J. Heeck, M. Holthausen, W. Rodejohann *et al*., Nucl. Phys. B **896**, 281 (2015), arXiv: 1412.3671[hep-ph]
[25] A. Crivellin, G. D'Ambrosio, and J. Heeck, Phys. Rev. D **91**(7), 075006 (2015), arXiv: 1503.03477[hep-ph]
[26] M. Ardu and F. Kirk, Eur. Phys. J. C **83**(5), 394 (2023), arXiv: 2205.02254[hep-ph]
[27] J. Heeck and W. Rodejohann, Phys. Rev. D **84**, 075007 (2011), arXiv: 1107.5238[hep-ph]
[28] T. Nomura and P. Sanyal, Phys. Rev. D **100**(11), 115036 (2019), arXiv: 1907.02718[hep-ph]
[29] U. Bellgardt *et al*. (SINDRUM), Nucl. Phys. B **299**, 1 (1988)
[30] B. Pontecorvo, Zh. Eksp. Teor. Fiz. **34**, 247 (1957)
[31] Z. Maki, M. Nakagawa, and S. Sakata, Prog. Theor. Phys. **28**, 870 (1962)
[32] S. Abe *et al*. (KamLAND-Zen), Phys. Rev. Lett. **130**(5), 051801 (2023), arXiv: 2203.02139[hep-ex]
[33] N. Abgrall *et al*. (LEGEND), AIP Conf. Proc. **1894**(1), 020027 (2017), arXiv: 1709.01980[physics.ins-det]
[34] J. B. Albert *et al*. (nEXO), Phys. Rev. C **97**(6), 065503 (2018), arXiv: 1710.05075[nucl-ex]